The EMBO Journal Vol. 21 No. 11 pp. 2557–2567, 2002

A tubular EHD1-containing compartment involved in the recycling of major histocompatibility complex class I molecules to the plasma membrane

Steve Caplan, Naava Naslavsky[1], Lisa M.Hartnell, Robert Lodge, Roman S.Polishchuk[2], Julie G.Donaldson[1] and Juan S.Bonifacino[3]

Cell Biology and Metabolism Branch, National Institute of Child Health and Human Development and [1]Laboratory of Cell Biology, National Heart Lung and Blood Institute, National Institutes of Health, Bethesda, MD 20892, USA and [2]Department of Cell Biology and Oncology, Istituto di Ricerche Farmacologiche 'Mario Negri', Consorzio Mario Negri Sud, Santa Maria Imbaro (Chieti), Italy

[3]Corresponding author
e-mail: juan@helix.nih.gov

The Eps15 homology (EH) domain-containing protein, EHD1, has recently been ascribed a role in the recycling of receptors internalized by clathrin-mediated endocytosis. A subset of plasma membrane proteins can undergo internalization by a clathrin-independent pathway regulated by the small GTP-binding protein ADP-ribosylation factor 6 (Arf6). Here, we report that endogenous EHD proteins, as well as transgenic tagged EHD1, are associated with long, membrane-bound tubules containing Arf6. EHD1 appears to induce tubule formation, which requires nucleotide cycling on Arf6 and intact microtubules. Mutations in the N-terminal P-loop domain or deletion of the C-terminal EH domain of EHD1 prevent association of EHD1 with tubules or induction of tubule formation. The EHD1 tubules contain internalized major histocompatibility complex class I (MHC-I) molecules that normally traffic through the Arf6 pathway. Recycling assays show that overexpression of EHD1 enhances MHC-I recycling. These observations suggest an additional function of EHD1 as a tubule-inducing factor in the Arf6 pathway for recycling of plasma membrane proteins internalized by clathrin-independent endocytosis.

Keywords: Arf6/clathrin-independent/EHD1/MHC class I/recycling

Introduction

Endocytic receptors such as the epidermal growth factor (EGF) receptor and the transferrin receptor contain signals within their cytoplasmic domains that mediate their rapid internalization from the plasma membrane (for reviews see Trowbridge *et al*., 1993; Bonifacino and Dell'Angelica, 1999). Internalization of these receptors is effected by a complex molecular machinery comprising clathrin and various clathrin-associated proteins (for reviews see Kirchhausen, 2000; Brodsky *et al*., 2001). These proteins assemble on the cytoplasmic face of the membrane to form a supramolecular complex known as a clathrin coat, which recruits the plasma membrane receptors by virtue of interactions with their endocytic signals. Clathrin-coated domains of the plasma membrane undergo invagination and eventually pinch off as clathrin-coated vesicles. These vesicles carry the internalized receptors to the early endosomal system, from where some receptors (e.g. the EGF receptor) are targeted to late endosomes and then lysosomes for degradation, while others (e.g. the transferrin receptor) are recycled back to the plasma membrane via a morphologically distinct organelle known as the endosomal recycling compartment (ERC) (for a review see Gruenberg and Maxfield, 1995).

Many other plasma membrane proteins lack conventional endocytic signals, but can nonetheless undergo internalization via clathrin-independent pathways (for a review see Nichols and Lippincott-Schwartz, 2001). The mechanisms involved in clathrin-independent endocytosis are not well understood. Among the mechanisms that have been invoked for this type of internalization are uptake through non-coated invaginations of the membrane known as caveolae (Kurzchalia and Parton, 1999), endocytosis via lipid rafts (Nichols *et al*., 2001), micropinocytosis (Lamaze and Schmid, 1995) and macropinocytosis (Hewlett *et al*., 1994). The endocytosis of the bulk of plasma membrane proteins devoid of conventional endocytic signals, such as the interleukin-2 (IL-2) receptor α subunit (Tac), class I molecules of the major histocompatibility complex (MHC-I), β1-integrin, CD1a, plakoglobin and cadherins, appears to occur along a pathway regulated by the small GTP-binding protein ADP-ribosylation factor 6 (Arf6) (Radhakrishna and Donaldson, 1997; Sugita *et al*., 1999; Brown *et al*., 2001). Hydrolysis of GTP on Arf6 is required for completion of the internalization step, while exchange of GTP for GDP allows for the return of the internalized proteins to the plasma membrane. The proteins internalized by this pathway have been shown to pass through a tubular endosomal compartment distinct from the ERC on their way back to the plasma membrane (Radhakrishna and Donaldson, 1997).

The molecular mechanisms involved in the recycling of proteins internalized by either clathrin-dependent or clathrin-independent endocytosis remain to be elucidated. Recently, a protein known as RME-1 in *Caenorhabditis elegans* and its human ortholog, EHD1, have been implicated in the return to the cell surface of proteins internalized by clathrin-dependent endocytosis (Grant *et al*., 2001; Lin *et al*., 2001). EHD1 is one of four closely related paralogs expressed ubiquitously in human cells, the other three being EHD2, EHD3 and EHD4 (Mintz *et al*., 1999; Pohl *et al*., 2000). All members of this family comprise three domains: an N-terminal P-loop domain containing nucleotide-binding motifs; a central region with high probability of forming coiled coils; and a

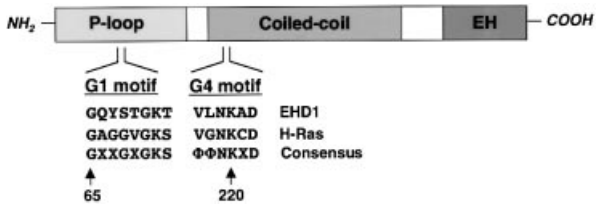

Fig. 1. EHD1 domain organization and homology to GTP-binding proteins. A schematic representation of human EHD1. EHD1 comprises an N-terminal P-loop, a central coiled coil and a C-terminal EH domain. EHD1 motifs that conform to polypeptide loops involved in GTP binding are shown at amino acids 65–72 (G1) and 217–222 (G4). Note that G2 and G5 motifs (which are more heterogeneous) have not been identified in EHD1, and a sequence with low homology to the G3 motif consensus is found between amino acids 351 and 358 (data not shown). The G1 and G4 amino acid sequences of EHD1 are aligned with those of the GTP-binding protein H-Ras, and with a consensus sequence for Ras-family GTP-binding motifs. X represents any amino acid; Φ represents a bulky hydrophobic amino acid.

C-terminal Eps15-homology (EH) domain (Mintz *et al*., 1999; Pohl *et al*., 2000; Figure 1). Mutation or RNAi-mediated interference of RME-1 in *C.elegans* inhibited the uptake of yolk protein bound to the vitellogenin receptor in developing oocytes (Grant *et al*., 2001), a process known to be dependent on clathrin (Grant and Hirsh, 1999). This endocytic defect seemed to be secondary to an inability to recycle internalized proteins from the ERC to the plasma membrane (Grant *et al*., 2001). Experiments using expression of a dominant-negative EHD1 construct in Chinese hamster ovary (CHO) cells provided additional evidence for a role of EHD1 in recycling to the plasma membrane. The mutant EHD1 was found to cause dispersal of the ERC and inhibition of transferrin receptor recycling to the plasma membrane (Lin *et al*., 2001). Thus, EHD1 is likely to be a component of the molecular machinery responsible for the return of endocytic receptors to the plasma membrane. A role for EHD1 in the regulation of signaling by insulin-like growth factor receptor 1 has also been proposed (Rotem-Yehudar *et al*., 2001). The possible involvement of EHD1 in the recycling of membrane proteins internalized by clathrin-independent pathways, however, remains to be investigated.

Here we show that endogenous EHD1 and Myc-epitope- or GFP-tagged EHD1 expressed by transfection into various cell lines localize to an array of long tubular structures emanating from the juxtanuclear area towards the periphery of the cells. The tubules themselves are relatively stable, although the association of EHD1 with them is dynamic. Mutations in the predicted nucleotide-binding region or deletion of the EH domain of EHD1 prevent its association with the tubules. Interference with the Arf6 GTP–GDP cycle causes disruption of the EHD1-containing tubules. Moreover, the tubules contain associated Arf6 and internalized MHC-I being recycled to the plasma membrane. Finally, overexpression of EHD1 enhances the rate of MHC-I recycling to the plasma membrane. These observations indicate that EHD1 participates in the Arf6-regulated pathway for the recycling of plasma membrane proteins internalized by clathrin-independent endocytosis. Thus, EHD1 may be involved in various pathways of protein recycling to the plasma membrane.

Results

Association of EHD1 with cytoplasmic tubules

To address the role of EHD1 in clathrin-independent endocytosis and recycling, we utilized HeLa cells, which have been shown to maintain distinct recycling compartments for proteins internalized by clathrin-dependent and -independent endocytosis (Radhakrishna and Donaldson, 1997; N.Naslavsky, R.Weigert and J.G.Donaldson, submitted). The expression and distribution of EHD proteins in HeLa cells was assessed using a polyclonal antibody to recombinant EHD1. This antibody is likely to recognize all four members of this family in human cells (EHD1–4), due to their high degree of sequence identity (Pohl *et al*., 2000). Untransfected HeLa cells (Figure 2A, PI and UT) or HeLa cells transfected with a construct encoding GFP–EHD1 (Figure 2A, T) were subjected to SDS–PAGE and immunoblot analysis using either the anti-EHD1 antibody (Figure 2A, UT and T) or pre-immune serum (Figure 2A, PI). In untransfected cells, the anti-EHD1 antibody detected a species of 55 kDa, which corresponded approximately to the predicted molecular mass of the endogenous EHD proteins. Accordingly, monomeric EHD proteins would be expected to migrate with a sedimentation coefficient similar to that of albumin, at ~4.6S. However, sedimentation velocity analyses revealed that the native EHD proteins migrated as much larger species of over 11.3S (Figure 2B), indicating that these proteins exist as subunits of oligomeric complexes. In immunoblots of HeLa cells transfected with the GFP–EHD1 construct (Figure 2A, T), we observed an additional species of 85 kDa, which corresponded to the expected molecular mass of the fusion protein. Based on an average transfection efficiency of ~60%, the level of GFP–EHD1 expression (85 kDa band) relative to endogenous EHD proteins (55 kDa band) per cell was estimated at 5- to 10-fold in several experiments. No bands were detected when immunoblotting was performed with pre-immune serum (Figure 2A, PI), thus confirming that the anti-EHD1 antibody specifically recognized endogenous EHD proteins as well as transgenic GFP–EHD1.

Myc-EHD1 (Figure 2C) or GFP–EHD1 (Figure 2D) expressed by transfection in HeLa cells was localized to a concentration of vesicles in the juxtanuclear area of the cell, as previously reported for endogenous EHD proteins in CHO cells (Lin *et al*., 2001). More strikingly, however, we also observed staining of an extensive array of thick tubules reaching lengths of up to 10 μm. Similar tubules were observed in COS-7 or M1 cells expressing GFP–EHD1, and shorter, less abundant tubular structures could also be discerned in CHO-1 cells, in addition to the more vesicular pattern (data not shown). Untransfected HeLa cells immunostained for endogenous EHD proteins also displayed cytoplasmic tubules (Figure 2E–G), although these were less numerous and fainter than in the transfected cells. Staining of these EHD-containing tubules was competed by the addition of recombinant GST–EHD1 (data not shown), thus demonstrating the specificity of EHD protein immunodetection. The prominence of tubular staining in the transfected cells is likely to be due to an enhancement of tubule formation by expression of the EHD1 fusion proteins.

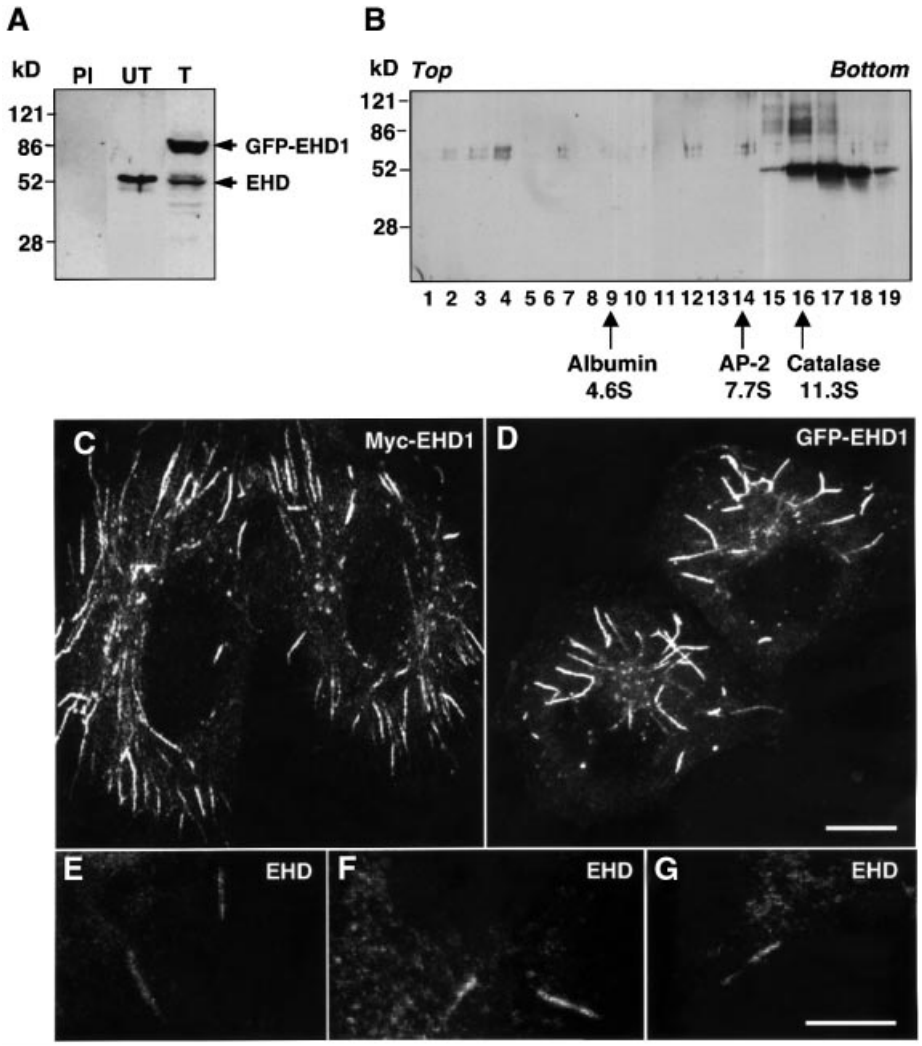

Fig. 2. EHD1 localizes to an array of long tubular structures. (**A**) Detergent lysates were prepared from untransfected HeLa cells (PI and UT) or HeLa cells transfected with a GFP–EHD1 construct (T), and resolved by 4–20% SDS–PAGE. Immunoblot analysis with either pre-immune serum (PI) or rabbit polyclonal antibody directed against EHD1 (UT and T) revealed the presence of both endogenous EHD1 (55 kDa) and transgenic GFP–EHD1 (85 kDa) proteins. Following transient transfection, ~60% of the cells expressed detectable levels of EHD1, and the relative levels of transfected and endogenous proteins were estimated by densitometric analysis of multiple film exposures. (**B**) HeLa cell extracts were subjected to sedimentation velocity analysis on a 4–20% sucrose gradient. Fractions were collected, resolved by 4–20% SDS–PAGE, and proteins were visualized by immunoblot analysis using the polyclonal antibody prepared against EHD1. Size markers indicate the positions of albumin, AP-2 complex and catalase on the sucrose gradients. (**C**) HeLa cells were transfected with a plasmid encoding Myc-EHD1. Cells were fixed and permeabilized 24 h later, and incubated with a mouse monoclonal antibody to the Myc epitope. Bound antibodies were revealed by incubation with Cy3-conjugated donkey anti-mouse IgG, demonstrating the presence of a dense network of Myc-EHD1 tubular organelles. (**D**) HeLa cells were transfected with a plasmid encoding GFP–EHD1, and were fixed and permeabilized after 24 h. (**E–G**) Untransfected HeLa cells were fixed, permeabilized and incubated with a rabbit polyclonal antibody to endogenous EHD1. Bound antibodies were revealed by incubation with Cy3-conjugated donkey anti-rabbit IgG. Images show the presence of long, tubular structures containing endogenous EHD proteins. All images were obtained by confocal microscopy. Bars: (C and D), 10 μm; (E–G), 10 μm.

Tubules containing associated EHD1 are membrane-bound organelles

To determine whether EHD1 tubular structures were membrane-bound organelles or exclusively protein assemblies, we performed immunoelectron microscopy of ultrathin frozen sections of HeLa cells expressing Myc-EHD1. Immunogold staining for EHD1 revealed labeling of many round and ellipsoidal structures that were clearly delimited by a membrane. Figure 3A shows a section of a tubular structure of ~260 nm diameter labeled for Myc-EHD1. To establish further the correspondence of the tubular structures observed by light microscopy with the membrane-bound organelles observed by electron microscopy, we performed correlative fluorescence electron microscopy as described previously (Polishchuk *et al.*, 2000). Figure 3B shows a confocal fluorescence image of a live HeLa cell expressing GFP–EHD1, with the typical array of EHD1 tubules extending throughout the cytoplasm. The exact same tubule depicted in the box in Figure 3B was examined by immunoelectron microscopy of serial sections, two of which are shown in Figure 3C and D. This tubule containing associated GFP–EHD1, as labeled by the enhanced gold particles, was found to be a membrane-bound structure of ~220 nm in diameter. The specificity of the staining can be appreciated by the absence of label on the adjacent mitochondria (M).

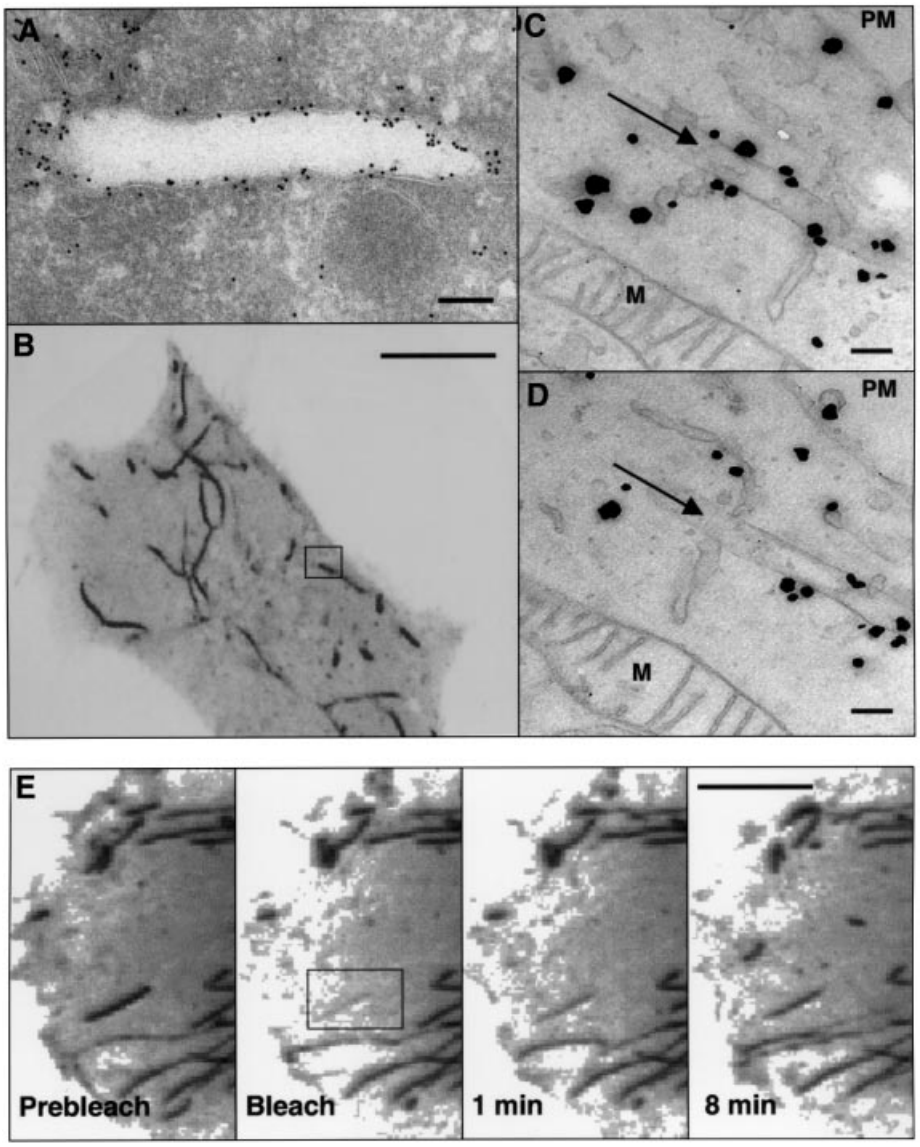

Fig. 3. Ultrastructural analysis of EHD1 tubules. (**A**) HeLa cells were transiently transfected with Myc-EHD1 and processed for electron microscopy immunogold labeling using an anti-Myc antibody. Bound antibodies were detected using gold-conjugated protein A. (**B**–**D**) Correlative fluorescence/electron microscopy. HeLa cells were transiently transfected with a GFP–EHD1 construct on CELLocate grids, and live confocal images of a typical GFP–EHD1-expressing cell were obtained (B). Cells were then fixed with 4% paraformaldehyde and 0.05% glutaraldehyde, and enhanced gold labeling was performed for anti-GFP antibodies as described in Materials and methods. (C) and (D) are serial sections depicting the boxed region of interest in (B), and arrows in (C) and (D) mark the EHD1 tubular structure within the box. Particles indicate the presence of GFP–EHD1 along the tubular structure and in the cytosol. (**E**) Dynamics of EHD1 association with membranes. GFP–EHD1 was subjected to fluorescence recovery after photobleaching (FRAP) analysis. HeLa cells were transiently transfected with a GFP–EHD1 construct, and examined by live confocal image analysis 24 h later. An entire EHD1 tubular structure was photobleached (rectangular region of interest). GFP–EHD1 recovery to the bleached area was monitored every 3.3 s (see Supplementary time-lapse video). Images of live cells (B and E) are visualized as inverted images to facilitate analysis. M, mitochondria; PM, plasma membrane. Bars: (A), 200 nm; (B), 10 μm; (C and D), 200 nm; (E), 10 μm.

To examine the dynamics of GFP–EHD1 tubules *in vivo*, transfected HeLa cells were monitored by time-lapse confocal image analysis. Long GFP–EHD1 tubular structures were quite stable and exhibited only limited movement over a 2 h period, although smaller tubular and vesicular structures were more mobile and in some cases could be seen fusing with the plasma membrane (data not shown). After photobleaching an entire GFP–EHD1 tubule (black box in Figure 3E and Supplementary video available at *The EMBO Journal* Online), its fluorescence recovered within minutes, indicating that GFP–EHD1 is continuously cycling on and off the tubules.

Structural requirements of EHD1 for tubule formation

The previously reported mutation of glycine 65 to arginine in the P-loop domain of EHD1 (Grant *et al*., 2001; Lin *et al*., 2001; Figure 1, G1 motif), which would be expected to disrupt nucleotide binding, rendered the GFP–EHD1 fusion protein cytosolic (Figure 4B). Similarly, mutation of lysine 220 to asparagine, within another stretch of amino acid residues with homology to GTP-binding proteins (Figure 1, G4 motif), also yielded a cytosolic protein (Figure 4C). Truncation of the C-terminal EH domain, on the other hand, resulted in a protein that

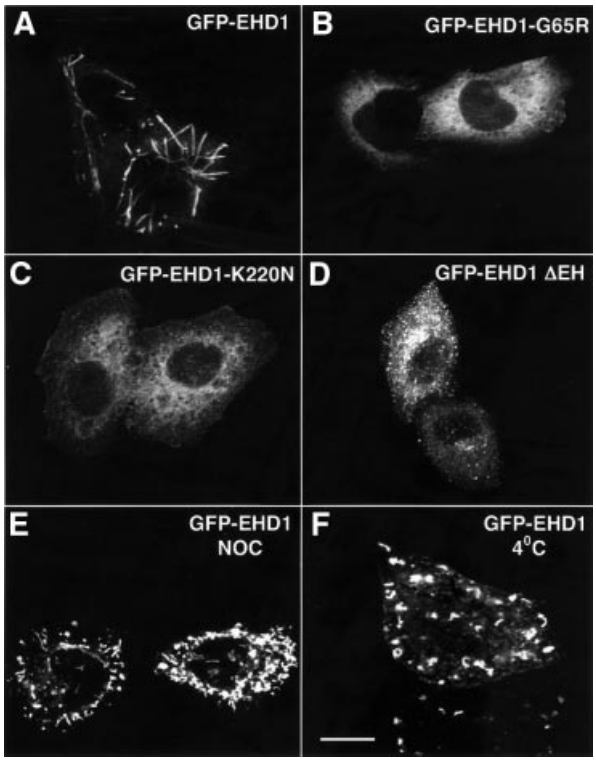

Fig. 4. Requirements for EHD1 tubule formation. HeLa cells were transiently transfected with cDNA constructs coding for wild-type GFP–EHD1 (**A**), GFP–EHD1-G65R (**B**), GFP–EHD1-K220N (**C**), or GFP–EHD1 ΔEH (**D**), fixed 24 h later, and analyzed by confocal microscopy. Wild-type GFP–EHD1-transfected HeLa cells were also treated for 1.5 h with nocodazole (NOC) (**E**), or maintained at 4°C for 1 h (**F**) prior to fixation. Images were obtained by confocal microscopy. Bar, 10 μm.

associated with membranes, but gave a vesicular rather than tubular pattern of staining (Figure 4D). Thus, the nucleotide-binding site in the P-loop appears to be required for association with membranes, while the EH domain is required for association with, or induction of, tubules.

To determine whether EHD1 tubular membrane structures are supported by components of the cytoskeleton, we treated cells with various inhibitors. The actin-depolymerizing agent cytochalasin D had no effect on the formation of EHD1 tubular structures (data not shown). In contrast, the microtubule-depolymerizing agent nocodazole (NOC) caused fragmentation of the tubules (Figure 4E). Similarly, incubation at 4°C, which is known to disrupt microtubules but not actin microfilaments, caused fragmentation of the tubules (Figure 4F). These results suggest that microtubules are necessary for the formation of EHD1 tubular profiles, possibly serving as a scaffold for their assembly.

Arf6 co-localizes with EHD1 and regulates the formation of EHD1-containing tubules

The long tubules observed in EHD1-transfected cells are reminiscent of tubular endosomes in the Arf6-regulated recycling pathway (Radhakrishna and Donaldson, 1997; Brown *et al*., 2001). Co-expression of normal Arf6 together with Myc-EHD1 revealed that both proteins indeed co-localized to the same tubular structures (Figure 5A–C, arrows). To determine whether the nucleotide status of Arf6 affected the EHD1 tubules, GFP–EHD1 was co-expressed with the GTP-locked Arf6-Q67L mutant (Peters *et al*., 1995; Radhakrishna and Donaldson, 1997) or the GDP-locked Arf6-T27N mutant (D'Souza-Schorey *et al*., 1995; Radhakrishna and Donaldson, 1997). As shown in Figure 5, expression of Arf6-Q67L (Figure 5D–F) abrogated the formation of EHD1 tubular structures. Although some peripheral co-localization was observed between Arf6-T27N and remnants of EHD1 tubules (Figure 5G–I), overall the expression of Arf6-T27N impaired the association of EHD1 with its characteristic tubules, often inducing the fragmentation of these structures. However, mutant EHD1 proteins did not affect the normal distribution pattern of Arf6 (data not shown). These observations suggest that cycling of Arf6 between its GTP- and GDP-bound states is necessary for either association of EHD1 with tubules or the formation of the tubules themselves. Expression of EFA6, a GTP-exchange factor for Arf6 (Franco *et al*., 1999; Figure 5J–L), or ACAP1, a GTPase-activating protein for Arf6 (Jackson *et al*., 2000; Figure 5M–O), caused fragmentation or disorganization of the tubules, although the effects were less dramatic than those observed upon expression of the Arf6-Q67L or Arf6-T27N constructs.

The specificity of Arf6 effects on EHD1 tubular structures was examined by assessing the effects of other GTP-binding proteins on EHD1 tubule formation. Neither GTP- nor GDP-locked mutants of Arf1 (Arf1-Q71L and Arf1-T31N, respectively) affected the EHD1 tubules (data not shown). Similarly, GTP- and GDP-locked mutants of Arf4 lacked any visible effect on EHD1 tubes (data not shown), suggesting that Arf6 is likely to be the only Arf family member that functionally interacts with EHD1. Moreover, the GTP-binding proteins Rab5 and Rab11, implicated in endocytosis and recycling in the clathrin-dependent pathway (Sheff *et al*., 1999; Sonnichsen *et al*., 2000; McCaffrey *et al*., 2001), were found to lack any effect on EHD1 tubules (data not shown). Overall, these results indicate that Arf6 and EHD1 functionally interact on the cytoplasmic tubular compartment.

A role for EHD1 in recycling MHC-I to the cell surface

Arf6-regulated tubular endosomes have been shown to contain recycling MHC-I molecules (Radhakrishna and Donaldson, 1997; N.Naslavsky, R.Weigert and J.G.Donaldson, submitted). The main function of MHC-I molecules is to bind endogenous antigenic peptides in the endoplasmic reticulum (ER) for presentation on the surface of the cells to $CD8^+$ T lymphocytes (for a review see Natarajan *et al*., 1999). Surface MHC-I molecules, however, can also undergo endocytosis by clathrin-independent mechanisms (Radhakrishna and Donaldson, 1997) and acquire peptides within endosomes (Dasgupta *et al*., 1988; Reid and Watts, 1990; Schirmbeck and Reimann, 1996; Gromme *et al*., 1999). We hypothesized that, along with Arf6, EHD1 might be involved in recycling of internalized MHC-I molecules to the cell surface. To test this hypothesis, HeLa cells expressing GFP–EHD1 were allowed to internalize for 30 min an antibody that recognizes peptide-loaded MHC-I. The cells were acid

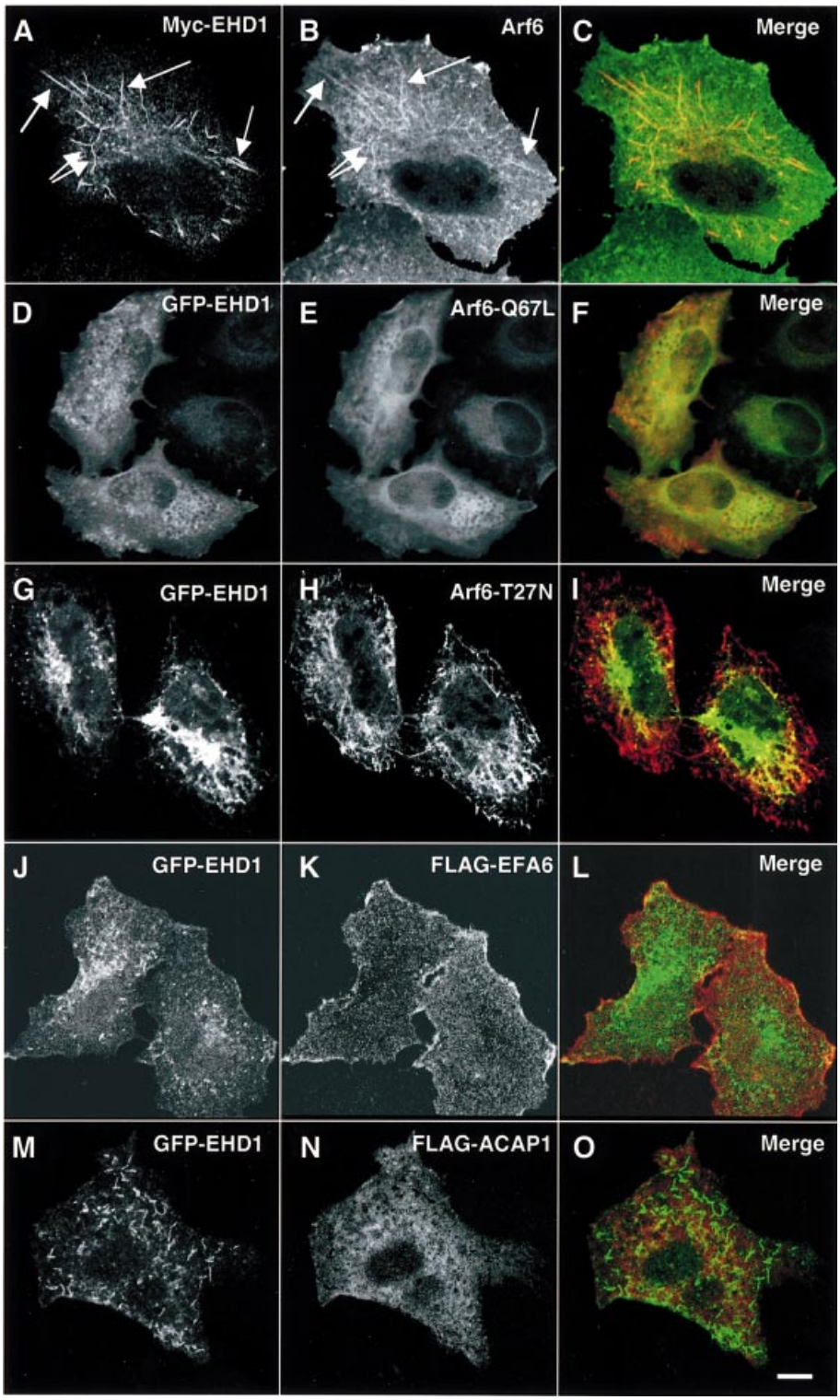

Fig. 5. Co-localization and functional interaction of EHD1 with Arf6. HeLa cells were transiently co-transfected with constructs encoding Myc-EHD1 and wild-type Arf6 (**A–C**), GFP–EHD1 and Arf6-Q67L (**D–F**), GFP–EHD1 and Arf6-T27N (**G–I**), GFP–EHD1 and FLAG-EFA6 (**J–L**), and GFP–EHD1 and FLAG-ACAP1 (**M–O**). Cells were fixed, permeabilized and incubated with a monoclonal antibody to the Myc epitope and a rabbit polyclonal antibody to Arf6 (A–C). Bound antibodies were revealed by Alexa-488-conjugated antibody to mouse IgG (A and C), and by Cy3-conjugated anti-rabbit IgG (B and C). HeLa cells co-transfected with GFP–EHD1 and Arf6 mutant constructs (D–I) were fixed, permeabilized and incubated with a rabbit polyclonal antibody directed against Arf6 (D–I), followed by Cy3-conjugated anti-rabbit IgG (E, F, H and I). HeLa cells co-transfected with GFP–EHD1 and FLAG-EFA6 (J–L) or FLAG-ACAP1 (M–O) were fixed, permeabilized and incubated with a monoclonal antibody to the FLAG epitope, followed by a Cy3-conjugated anti-mouse IgG antibody. All images were obtained by confocal microscopy. Arrows (A and B) denote tubular structures containing both Arf6 and EHD1. Bar, 10 μm.

rinsed to remove surface-bound antibodies, then fixed and permeabilized, and finally decorated with a fluorescently labeled secondary antibody to reveal internalized MHC-I. Internalization of MHC-I appeared normal in GFP–EHD1-expressing cells as compared with untransfected cells. Interestingly, internalized MHC-I was often found in beaded tubular endosomes, some of which contained associated GFP–EHD1 (Figure 6A–F, arrows). To examine further the partial co-localization of EHD1 and MHC-I at the ultrastructural level, HeLa cells were co-transfected with Myc-EHD1 and mouse MHC-I (H-2D^d), and the cells were continuously incubated with anti-H-2D^d antibody (which recognizes peptide-loaded mouse MHC-I) for 50 min, followed by fixation and processing for immunoelectron microscopy. In agreement with data from indirect immunofluorescence microscopy, a portion of the tubular and vesicular membrane-bound structures observed contained both Myc-EHD1 and internalized MHC-I. The membrane-bound structure depicted in Figure 6G is an example of such a tubule containing Myc-EHD1 (Figure 6G; 15 nm gold particles) and internalized MHC-I (Figure 6G; 10 nm gold particles).

To examine the kinetics with which internalized MHC-I enters the EHD1-containing tubular structures *in vivo*, we performed dual-color time-lapse confocal microscopy of MHC-I antibody uptake in comparison with GFP–EHD1. GFP–EHD1-transfected HeLa cells were allowed to continuously internalize a mouse anti-MHC-I antibody pre-bound to a fluorescently conjugated anti-mouse Fab fragment, and confocal images were acquired every 6 s. Within 5 min of uptake, internalized MHC-I appeared mostly in punctate structures that showed little or no co-localization with the GFP–EHD1 tubules (Figure 7A; Supplementary video). After 7 min and 42 s, some MHC-I began to appear in GFP–EHD1 tubular structures. However, the most extensive co-localization was evident after 16 min and 18 s (Figure 7A, arrows). These experiments indicated that MHC-I gained access to EHD1 tubules after 7–16 min of internalization, suggesting a role for the EHD1 tubules in recycling internalized MHC-I to the plasma membrane.

To assess the affect of EHD1 overexpression on the recycling of internalized MHC-I to the plasma membrane, we designed a 'CELISA' assay (N.Naslavsky, R.Weigert

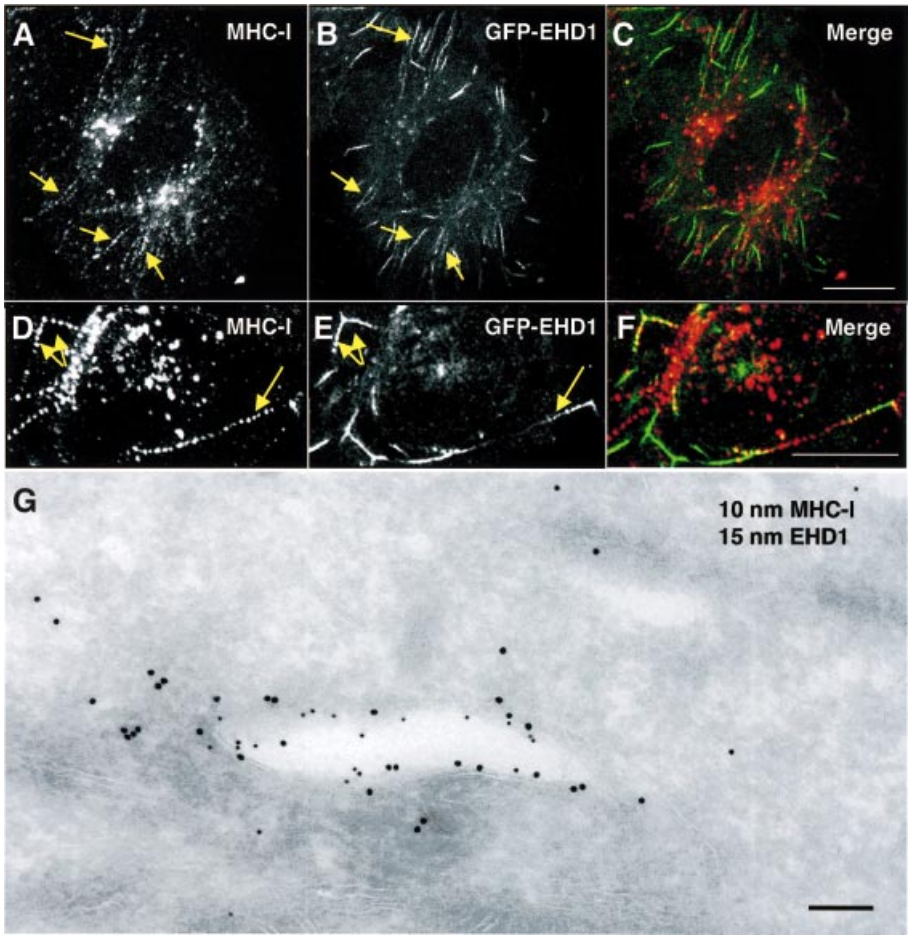

Fig. 6. Co-localization of EHD1 and internalized MHC-I molecules. (**A**–**F**) Co-localization of internalized MHC-I with EHD1 tubular structures. HeLa cells were transiently transfected with a construct encoding GFP–EHD1. After 24 h, the cells were continuously pulsed with W6/32 anti-MHC-I monoclonal antibody for 30 min. After brief acid washing to remove surface-bound MHC-I antibody, fixed and permeabilized cells were incubated with Cy3-conjugated anti-mouse IgG, and examined by confocal microscopy. Internalized MHC-I is shown in (A) and (D), and GFP–EHD1 is depicted in (B) and (E). (C and F) Merged images. (**G**) HeLa cells were transiently co-transfected with Myc-EHD1 and H-2D^d (mouse MHC-I) constructs. Cells were pulsed with anti-H-2D^d antibody 24 h later, fixed and processed for ultrathin section electron microscopy. EHD1 is marked by 15 nm gold particles, and 10 nm gold particles mark the presence of internalized H-2D^d. Arrows denote tubular structures positive for internalized MHC-I (A and D) and GFP–EHD1 (B and E). Bars: (A–C), 10 μm; (D–F), 10 μm; (G), 200 nm.

and J.G.Donaldson, submitted) that measures cell surface levels of MHC-I (Figure 7B). Since 4°C effectively disrupts EHD1 tubules, we were unable to utilize FACS analysis-based assays, which necessitate antibody binding on ice. Therefore, in our CELISA protocol, we allowed the binding of antibodies to MHC-I to proceed at 37°C for 5 min. During this pulse, MHC-I was internalized and the kinetics of peptide-bound MHC-I cell surface reappearance were monitored beginning after the initial MHC-I loading within the cell. HeLa cells were transfected with a mouse MHC-I construct (H-2D^d), or co-transfected with H-2D^d together with either normal or mutant EHD1 constructs. Since, on average, ~50% of the cells were transfected with EHD1, co-transfection of mouse MHC-I

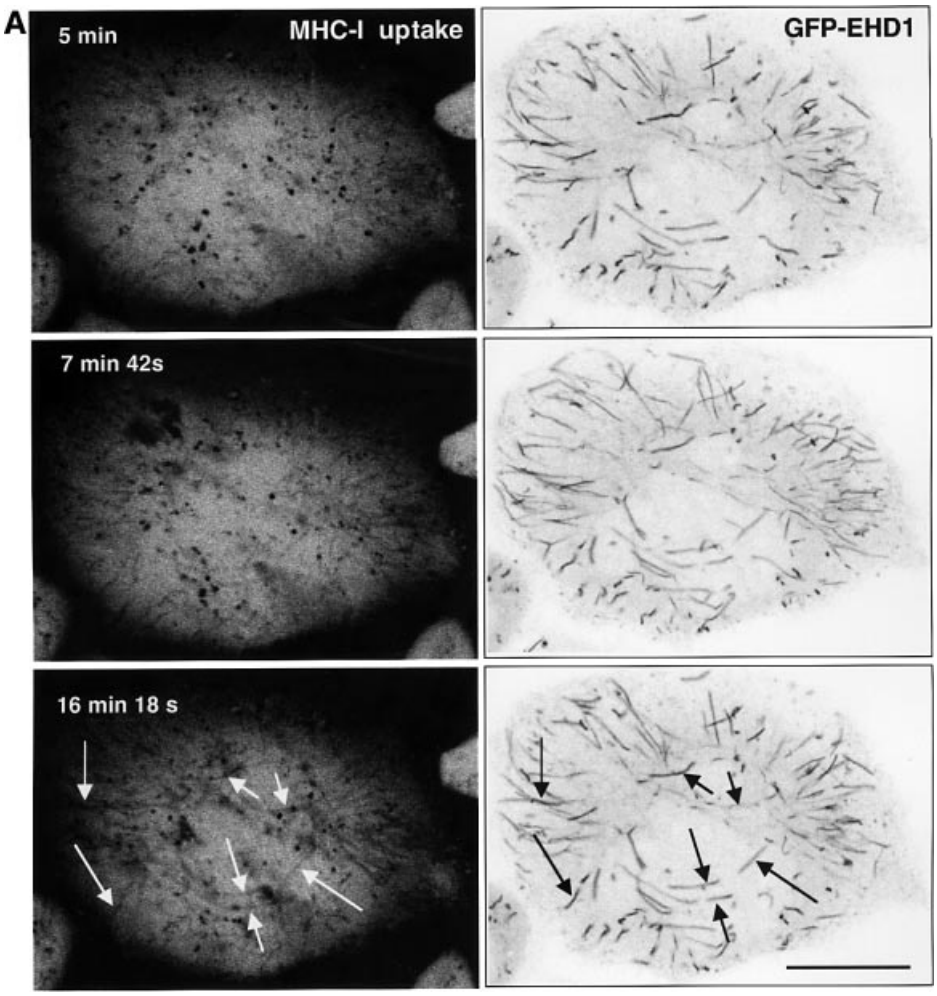

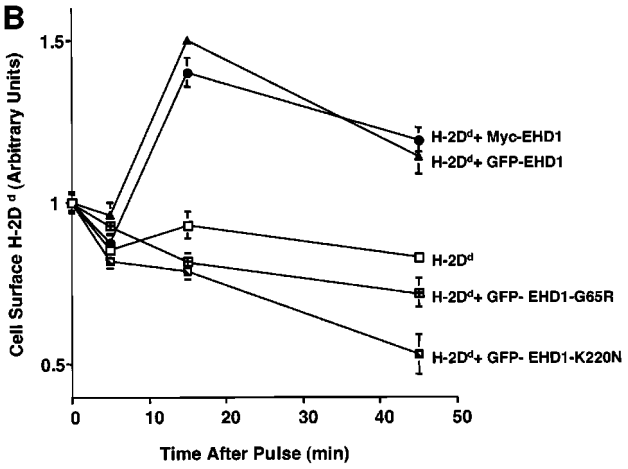

Fig. 7. EHD1 tubular structures promote recycling of MHC-I to the cell surface. (**A**) Time-dependent co-localization of internalized MHC-I with EHD1 tubules by live image analysis. MHC-I monoclonal antibodies were coupled to Alexa Fluor 568 F(ab′)2 fragment of goat anti-mouse IgG. The coupled antibodies were then used to continuously pulse HeLa cells that were transfected 24 h earlier with a GFP–EHD1 construct. Images of MHC-I uptake (left panels) and GFP–EHD1 tubules (right panels) are depicted. Arrows (white) mark MHC-I tubular structures that appear at 15–20 min of internalization and co-localize with pre-existing GFP–EHD1 tubules (black arrows). Images are shown inverted to facilitate analysis (see Supplementary time-lapse video). Bar, 10 μm. (**B**) Quantification of EHD1-enhanced MHC-I recycling by a CELISA assay. HeLa cells were transfected with cDNA coding for H-2D^d (mouse MHC-I), H-2D^d and GFP–EHD1, H-2D^d and Myc-EHD1, H-2D^d and GFP–EHD1-G65R, or H-2D^d and GFP–EHD1-K220N. Internalization of MHC-I over time was monitored 24 h after transfection by CELISA utilizing a biotinylated anti-MHC-I antibody (see Materials and methods), and the fraction of MHC-I antibody on the surface at each time point was recorded. A representative experiment from four independent CELISA assays is depicted, with triplicates at each time point.

allowed analysis of MHC-I exclusively in cells overexpressing EHD1. Overexpression of either GFP–EHD1 or Myc-EHD1 enhanced the recycling of internalized H-2D^d to the cell surface, with a peak visible at 15 min after the pulse (the arbitrary unit 1 is defined as the amount of H-2D^d detected on the cell surface after the 5 min pulse at 37°C). Both single point mutations in the putative nucleotide-binding loops (G65R and K220N) prevented the enhanced recycling, reducing it to levels below those of the control (Figure 7B). These results are consistent with a role for EHD1 in the regulation of MHC-I recycling to the cell surface via a cytoplasmic tubular compartment.

Discussion

The results presented here indicate the existence of a tubular, membrane-bound compartment containing associated EHD1 and Arf6. Tubules containing endogenous EHD proteins could be observed in untransfected HeLa cells, although they were much more prominent in cells transfected with constructs encoding GFP- or epitope-tagged EHD1. It is likely that the 5- to 10-fold overexpression of the tagged EHD1 constructs achieved in the transfected cells enhances tubule formation, suggesting that EHD1 has an intrinsic ability to induce membrane tubulation *in vivo*.

Photobleaching analyses revealed that GFP–EHD1 association with the tubes is a dynamic process. Recovery of GFP–EHD1 on the tubules after photobleaching could be due to recruitment from a cytoplasmic pool, although we cannot rule out delivery by vesicular transport. The N-terminal P-loop domain appears to control recruitment of EHD1 to membranes. The P-loop and central coiled-coil regions contain at least three stretches of amino acid residues that resemble nucleotide-binding motifs (termed G1, G3 and G4) in GTP-binding proteins (Sprang, 1997). Mutations that disrupt the more conserved G1 or G4 motifs resulted in cytosolic localization of the mutant EHD1 proteins, suggesting that nucleotide binding might be important for EHD1 recruitment to membranes. However, our attempts to demonstrate binding of nucleotides to EHD1 have so far been unsuccessful.

Another distinctive feature of EHD1 is the presence of a C-terminal EH domain. EH domains bind NPF (asparagine-proline-phenylalanine) motifs present in various proteins involved in vesicular traffic (Di Fiore *et al*., 1997). We found that the EH domain of EHD1 interacts with the NPF motif-containing proteins epsin 1 (Chen *et al*., 1998) and stonin 2/stoned-B (Martina *et al*., 2001; Walther *et al*., 2001) in the yeast two-hybrid system (data not shown). It remains to be established, however, whether these proteins are physiological interaction partners for EHD1 in cells. Unlike the P-loop domain, the EH domain was not required for membrane association of EHD1, but seemed necessary for tubule formation. In the absence of its EH domain, EHD1 localized to vesicles. These observations suggest that biogenesis of EHD1 tubular organelles may be a two-step process, requiring the P-loop domain for membrane association and the EH domain for the induction of tubular structures.

Previous studies demonstrated an involvement of EHD1 in recycling receptors internalized by clathrin-dependent endocytosis (Grant *et al*., 2001; Lin *et al*., 2001). Our experiments suggest that EHD1 may also be involved in the recycling of proteins that are internalized independently of clathrin. In particular, EHD1 appears to participate in the Arf6-regulated pathway for bulk recycling of plasma membrane proteins through non-clathrin-coated intermediates (Peters *et al*., 2001). The morphological hallmark of this pathway is a system of long tubules through which recycling plasma membrane proteins devoid of conventional endocytic signals pass *en route* to the plasma membrane (Radhakrishna and Donaldson, 1997). Not only did EHD1 co-localize with Arf6 on these tubules, but also manipulation of the nucleotide status of Arf6 caused disruption of the EHD1 tubules, suggesting that nucleotide cycling specifically on Arf6 is required for EHD1 tubule formation.

Among the proteins that traffic through the Arf6 pathway are MHC-I molecules (Radhakrishna and Donaldson, 1997; Brown *et al*., 2001; N.Naslavsky, R.Weigert and J.G.Donaldson, submitted). We observed that MHC-I molecules were initially internalized into vesicular structures scattered throughout the cytoplasm. Within 15–20 min of internalization, however, MHC-I molecules appeared in the EHD1 tubular structures, suggesting that the tubular compartment plays a role late in recycling. Indeed, evidence obtained by CELISA assays demonstrated that enhanced tubule formation upon overexpression of full-length EHD1 correlated with recycling of MHC-I (Figure 7), as well as Tac (data not shown) to the plasma membrane.

What might be the physiological role of MHC-I recycling via Arf6-regulated EHD1 tubules? MHC-I has long been known to function in the presentation of endogenous antigenic peptides to CD8$^+$ T lymphocytes (Natarajan *et al*., 1999). The antigenic peptides are produced in the cytosol and loaded onto newly synthesized MHC-I molecules in the ER (Cresswell, 2000). The peptide-loaded MHC-I molecules then travel to the plasma membrane via the secretory pathway. However, recent studies indicate that MHC-I can also present peptides derived from exogenous antigens (for reviews see Jondal *et al*., 1996; Rock, 1996). This presentation could be mediated by internalization of either 'empty' MHC-I molecules (Abdel-Motal *et al*., 1995; Schirmbeck and Reimann, 1996) or peptide-loaded MHC-I molecules that exchange their peptides within endosomes (Dasgupta *et al*., 1988; Reid and Watts, 1990; Gromme *et al*., 1999). In either case, the MHC-I molecules carrying newly acquired peptides would be transported to the plasma membrane via the Arf6 pathway, along EHD1 tubules.

Tubular compartments have previously been shown to mediate the recycling of receptors and other transmembrane proteins to the plasma membrane (Yamashiro *et al*., 1984; Hopkins *et al*., 1990; Sakai *et al*., 1998; Casanova *et al*., 1999; Verges *et al*., 1999; de Figueiredo *et al*., 2001; Johnson *et al*., 2001). The ERC, in particular, comprises a collection of vesicles and tubules involved in the recycling of the transferrin receptor and other endocytic receptors to the plasma membrane (Yamashiro *et al*., 1984). EHD1 is associated with the ERC, where it participates in transferrin receptor recycling (Lin *et al*., 2001). Thus, EHD1 may play a general role in the formation of different

types of tubular intermediates that carry recycling proteins to the cell surface.

Materials and methods

Recombinant DNA constructs

Human EHD1 was obtained by RT–PCR utilizing mRNA from HeLa cells. Epitope tagging was performed by PCR amplification of the full-length human EHD1 using 5′ primers containing the nucleotide sequence of the Myc epitope and adding *Xho*I and *Eco*RI restriction sites. This product was cloned into a pcDL-Srα296 (pXS) mammalian expression vector. Human EHD1 was also cloned into the *Xho*I and *Eco*RI sites of the EGFPC3 vector (Clontech), with GFP at the N-terminus of the fusion protein. Single amino acid substitutions were generated in GFP–EHD1 to produce GFP–EHD1-G65R and GFP–EHD1-K220N, and a stop codon was introduced at amino acid 434 using the QuikChange site-directed mutagenesis kit (Stratagene, La Jolla, CA). Expression vectors for the wild type and both GTP- and GDP-locked forms of Arf6 have been described (Radhakrishna and Donaldson, 1997). FLAG-EFA6 and FLAG-ACAP1 (Jackson *et al*., 2000), and both GTP- and GDP-locked HA-Arf1 constructs (Peters *et al*., 1995) have also been described previously. The H-2D^d mouse MHC-I construct was a gift from Dr D.Margulies (National Institutes of Health, Bethesda, MD).

Antibodies

The following monoclonal antibodies were used: 9E10 and HA.11 antibodies to the Myc and HA epitopes, respectively (Covance); W6/32 antibody to human MHC-I (peptide-bound) (American Type Culture Collection); 34-5-8 antibody to H-2D^d (peptide-bound) (Pharmingen); 34-5-8 antibody conjugated to biotin (Cedarlane Laboratories Limited); M5 antibody to the FLAG epitope (Sigma-Aldrich); Cy3-conjugated anti-mouse and anti-rabbit IgG (Molecular Probes, Inc.); Alexa-488-conjugated antibody to mouse IgG (Molecular Probes, Inc.); and Alexa Fluor 568 F(ab′)2 fragment of goat anti-mouse IgG (Molecular Probes, Inc.). Polyclonal serum was prepared by immunizing rabbits with human EHD1 or Arf6 (Radhakrishna and Donaldson, 1997). Polyclonal antibodies to GFP were purchased from Molecular Probes, Inc.

Electron microscopy

For immunoelectron microscopy of ultrathin frozen sections, HeLa cells were transiently transfected, fixed as described (Caplan *et al*., 2001), prepared for ultrathin frozen sectioning, and immunolabeled by a standard technique (Slot *et al*., 1991). For correlative immunofluorescence/electron microscopy, cells were transfected on CELLocate grids. After imaging by confocal microscopy, cells were fixed and incubated with anti-GFP antibody (Polishchuk *et al*., 2000). Cells were then labeled with Fab fragments of secondary antibodies conjugated to 1.4 nm Nanogold particles (Nanoprobes, Inc.) and developed with the GoldEnhance kit (Nanoprobes, Inc.). Once labeled, the cells were post-fixed in OsO_4, dehydrated in alcohols and embedded in Epon. Ultrathin serial sections and frozen sections were cut on a Leica Ultracut-S ultra microtome and photographed on a Philips CM-10 transmission electron microscope.

Immunofluorescence and live imaging microscopy

For fixed image analysis, HeLa cells were grown on coverglasses and transfected using FUGENE-6 (Roche Molecular Biochemicals), and fixed with 4% v/v paraformaldehyde in phosphate-buffered saline (PBS). Fixed cells were then incubated with primary antibodies containing 0.1% saponin and 0.1% bovine serum albumin (BSA; w/v) for 1 h at room temperature. After washes in PBS, the cells were incubated with the appropriate fluorochrome-labeled secondary antibody mixture containing 0.1% saponin and 0.1% BSA (w/v) for 30 min at room temperature. Images were obtained on a Zeiss LSM 410 confocal microscope (Zeiss, Thornwood, NY), using a 63× 1.4NA objective with appropriate filters. For live cell imaging, cells were maintained at 37°C and analyzed with a Zeiss 510 confocal microscope (Zeiss) equipped with a 63× 1.4 NA objective. The laser excitation setting was maintained at 488 nm for GFP and 543 nm for rhodamine, with appropriate filter sets as supplied by the manufacturer. Dual-color imaging was obtained through the multichannel setting for optimal channel definition. For fluorescence recovery studies, the confocal pinhole was set fully open to collect fluorescence from the entire breadth of the cell, using a 25× 0.8 immersion corrected objective. Selective photobleaching was performed utilizing a minimum of 70 scans with the 488 nm laser line at full power, and recovery was then monitored at low intensity illumination. Images were analyzed with either Zeiss LSM software, or NIH Image software.

Measurement of recycling by CELISA

HeLa cells were plated in 24-well dishes (SonicSeal; Nalgene Nunc International) at a concentration of 100 000 cells/well and co-transfected 24 h later with a mouse MHC-I H-2D^d construct (0.2 μg DNA/well) in combination with the appropriate plasmid expression vectors to be assayed (0.2 μg DNA/well). Twenty-four hours after transfection, cells were kept at 37°C and incubated for 5 min with 150 μl/well monoclonal antibody to peptide-bound H-2D^d conjugated to biotin (Cedarlane Laboratories Ltd), diluted 1:30. Unbound antibody was rinsed, and cells were either fixed (2% paraformaldehyde v/v in PBS) immediately to measure initial surface-bound antibody, or transferred to complete media and maintained at 37°C for various times prior to fixation. Fixed cells were incubated with 0.1 μg/ml streptavidin–horseradish peroxidase (prepared in 5% BSA/PBS) at room temperature for 15 min in a volume of 200 μl/well, and washed extensively with PBS. Colorimetric reactions were developed with the TMB substrate kit (Pierce, Rockford, IL) according to the manufacturer's instructions and OD_{450} was measured. Experiments were performed in triplicate, with data presented as a percentage of the initial surface-bound antibody.

Other procedures

Immunoblot analysis (Caplan *et al*., 2000) and sedimentation analysis (Dell'Angelica *et al*., 1997) were performed as described previously.

Supplementary data

Supplementary data for this paper are available at *The EMBO Journal* Online.

Acknowledgements

The authors are grateful to Professor Mia Horowitz for kindly providing an antibody to endogenous EHD proteins, as well as for helpful discussions, and to Dr David Margulies for kindly providing the plasmid encoding H-2D^d. S.C. is the recipient of a long-term Human Frontiers Science Program Fellowship. R.S.P. is the recipient of an Alfredo Leonardi Fellowship for rare disease.

References

Abdel-Motal,U.M., Berg,L., Bengtsson,M., Dahmen,J., Kihlberg,J., Magnusson,G., Nilsson,U. and Jondal,M. (1995) Major histocompatibility complex class I binding glycopeptides for the estimation of 'empty' class I molecules. *J. Immunol. Methods*, **188**, 21–31.

Bonifacino,J.S. and Dell'Angelica,E.C. (1999) Molecular bases for the recognition of tyrosine-based sorting signals. *J. Cell Biol.*, **145**, 923–926.

Brodsky,F.M., Chen,C.Y., Knuehl,C., Towler,M.C. and Wakeham,D.E. (2001) Biological basket weaving: formation and function of clathrin-coated vesicles. *Annu. Rev. Cell Dev. Biol.*, **17**, 517–568.

Brown,F.D., Rozelle,A.L., Yin,H.L., Balla,T. and Donaldson,J.G. (2001) Phosphatidylinositol 4,5-bisphosphate and Arf6-regulated membrane traffic. *J. Cell Biol.*, **154**, 1007–1017.

Caplan,S., Dell'Angelica,E.C., Gahl,W.A. and Bonifacino,J.S. (2000) Trafficking of major histocompatibility complex class II molecules in human B-lymphoblasts deficient in the AP-3 adaptor complex. *Immunol. Lett.*, **72**, 113–117.

Caplan,S., Hartnell,L.M., Aguilar,R.C., Naslavsky,N. and Bonifacino, J.S. (2001) Human Vam6p promotes lysosome clustering and fusion *in vivo*. *J. Cell Biol.*, **154**, 109–122.

Casanova,J.E., Wang,X., Kumar,R., Bhartur,S.G., Navarre,J., Woodrum,J.E., Altschuler,Y., Ray,G.S. and Goldenring,J.R. (1999) Association of Rab25 and Rab11a with the apical recycling system of polarized Madin–Darby canine kidney cells. *Mol. Biol. Cell*, **10**, 47–61.

Chen,H., Fre,S., Slepnev,V.I., Capua,M.R., Takei,K., Butler,M.H., Di Fiore,P.P. and De Camilli,P. (1998) Epsin is an EH-domain-binding protein implicated in clathrin-mediated endocytosis. *Nature*, **394**, 793–797.

Cresswell,P. (2000) Intracellular surveillance: controlling the assembly of MHC class I-peptide complexes. *Traffic*, **1**, 301–305.

Dasgupta,J.D., Watkins,S., Slayter,H. and Yunis,E.J. (1988) Receptor-

like nature of class I HLA: endocytosis via coated pits. *J. Immunol.*, **141**, 2577–2580.
de Figueiredo,P., Doody,A., Polizotto,R.S., Drecktrah,D., Wood,S., Banta,M., Strang,M.S. and Brown,W.J. (2001) Inhibition of transferrin recycling and endosome tubulation by phospholipase A2 antagonists. *J. Biol. Chem.*, **276**, 47361–47370.
Dell'Angelica,E.C., Ohno,H., Ooi,C.E., Rabinovich,E., Roche,K.W. and Bonifacino,J.S. (1997) AP-3: an adaptor-like protein complex with ubiquitous expression. *EMBO J.*, **16**, 917–928.
Di Fiore,P.P., Pelicci,P.G. and Sorkin,A. (1997) EH: a novel protein–protein interaction domain potentially involved in intracellular sorting. *Trends Biochem. Sci.*, **22**, 411–413.
D'Souza-Schorey,C., Li,G., Colombo,M.I. and Stahl,P.D. (1995) A regulatory role for ARF6 in receptor-mediated endocytosis. *Science*, **267**, 1175–1178.
Franco,M., Peters,P.J., Boretto,J., van Donselaar,E., Neri,A., D'Souza-Schorey,C. and Chavrier,P. (1999) EFA6, a sec7 domain-containing exchange factor for ARF6, coordinates membrane recycling and actin cytoskeleton organization. *EMBO J.*, **18**, 1480–1491.
Grant,B. and Hirsh,D. (1999) Receptor-mediated endocytosis in the *Caenorhabditis elegans* oocyte. *Mol. Biol. Cell*, **10**, 4311–4326.
Grant,B., Zhang,Y., Paupard,M.C., Lin,S.X., Hall,D.H. and Hirsh,D. (2001) Evidence that RME-1, a conserved *C. elegans* EH-domain protein, functions in endocytic recycling. *Nature Cell Biol.*, **3**, 573–579.
Gromme,M., Uytdehaag,F.G., Janssen,H., Calafat,J., van Binnendijk,R.S., Kenter,M.J., Tulp,A., Verwoerd,D. and Neefjes,J. (1999) Recycling MHC class I molecules and endosomal peptide loading. *Proc. Natl Acad. Sci. USA*, **96**, 10326–10331.
Gruenberg,J. and Maxfield,F.R. (1995) Membrane transport in the endocytic pathway. *Curr. Opin. Cell Biol.*, **7**, 552–563.
Hewlett,L.J., Prescott,A.R. and Watts,C. (1994) The coated pit and macropinocytic pathways serve distinct endosome populations. *J. Cell Biol.*, **124**, 689–703.
Hopkins,C.R., Gibson,A., Shipman,M. and Miller,K. (1990) Movement of internalized ligand–receptor complexes along a continuous endosomal reticulum. *Nature*, **346**, 335–339.
Jackson,T.R., Brown,F.D., Nie,Z., Miura,K., Foroni,L., Sun,J., Hsu, V.W., Donaldson,J.G. and Randazzo,P.A. (2000) ACAPs are arf6 GTPase-activating proteins that function in the cell periphery. *J. Cell Biol.*, **151**, 627–638.
Johnson,A.O., Lampson,M.A. and McGraw,T.E. (2001) A di-leucine sequence and a cluster of acidic amino acids are required for dynamic retention in the endosomal recycling compartment of fibroblasts. *Mol. Biol. Cell*, **12**, 367–381.
Jondal,M., Schirmbeck,R. and Reimann,J. (1996) MHC class I-restricted CTL responses to exogenous antigens. *Immunity*, **5**, 295–302.
Kirchhausen,T. (2000) Clathrin. *Annu. Rev. Biochem.*, **69**, 699–727.
Kurzchalia,T.V. and Parton,R.G. (1999) Membrane microdomains and caveolae. *Curr. Opin. Cell Biol.*, **11**, 424–431.
Lamaze,C. and Schmid,S.L. (1995) The emergence of clathrin-independent pinocytic pathways. *Curr. Opin. Cell Biol.*, **7**, 573–580.
Lin,S.X., Grant,B., Hirsh,D. and Maxfield,F.R. (2001) Rme-1 regulates the distribution and function of the endocytic recycling compartment in mammalian cells. *Nature Cell Biol.*, **3**, 567–572.
Martina,J.A., Bonangelino,C.J., Aguilar,R.C. and Bonifacino,J.S. (2001) Stonin 2: an adaptor-like protein that interacts with components of the endocytic machinery. *J. Cell Biol.*, **153**, 1111–1120.
McCaffrey,M.W., Bielli,A., Cantalupo,G., Mora,S., Roberti,V., Santillo,M., Drummond,F. and Bucci,C. (2001) Rab4 affects both recycling and degradative endosomal trafficking. *FEBS Lett.*, **495**, 21–30.
Mintz,L., Galperin,E., Pasmanik-Chor,M., Tulzinsky,S., Bromberg,Y., Kozak,C.A., Joyner,A., Fein,A. and Horowitz,M. (1999) EHD1—an EH-domain-containing protein with a specific expression pattern. *Genomics*, **59**, 66–76.
Natarajan,K., Li,H., Mariuzza,R.A. and Margulies,D.H. (1999) MHC class I molecules, structure and function. *Rev. Immunogenet.*, **1**, 32–46.
Nichols,B.J. and Lippincott-Schwartz,J. (2001) Endocytosis without clathrin coats. *Trends Cell Biol.*, **11**, 406–412.
Nichols,B.J., Kenworthy,A.K., Polishchuk,R.S., Lodge,R., Roberts,T.H., Hirschberg,K., Phair,R.D. and Lippincott-Schwartz,J. (2001) Rapid cycling of lipid raft markers between the cell surface and Golgi complex. *J. Cell Biol.*, **153**, 529–541.
Peters,P.J., Hsu,V.W., Ooi,C.E., Finazzi,D., Teal,S.B., Oorschot,V., Donaldson,J.G. and Klausner,R.D. (1995) Overexpression of wild-type and mutant ARF1 and ARF6: distinct perturbations of nonoverlapping membrane compartments. *J. Cell Biol.*, **128**, 1003–1017.
Peters,P.J., Gao,M., Gaschet,J., Ambach,A., van Donselaar,E., Traverse,J.F., Bos,E., Wolffe,E.J. and Hsu,V.W. (2001) Characterization of coated vesicles that participate in endocytic recycling. *Traffic*, **2**, 885–895.
Pohl,U. *et al*. (2000) EHD2, EHD3 and EHD4 encode novel members of a highly conserved family of EH domain-containing proteins. *Genomics*, **63**, 255–262.
Polishchuk,R.S., Polishchuk,E.V., Marra,P., Alberti,S., Buccione,R., Luini,A. and Mironov,A.A. (2000) Correlative light-electron microscopy reveals the tubular–saccular ultrastructure of carriers operating between Golgi apparatus and plasma membrane. *J. Cell Biol.*, **148**, 45–58.
Radhakrishna,H. and Donaldson,J.G. (1997) ADP-ribosylation factor 6 regulates a novel plasma membrane recycling pathway. *J. Cell Biol.*, **139**, 49–61.
Reid,P.A. and Watts,C. (1990) Cycling of cell-surface MHC glycoproteins through primaquine-sensitive intracellular compartments. *Nature*, **346**, 655–657.
Rock,K.L. (1996) A new foreign policy: MHC class I molecules monitor the outside world. *Immunol. Today*, **17**, 131–137.
Rotem-Yehudar,R., Galperin,E. and Horowitz,M. (2001) Association of insulin-like growth factor 1 receptor with EHD1 and SNAP29. *J. Biol. Chem.*, **276**, 33054–33060.
Sakai,T., Mizuno,T., Miyamoto,H. and Kawasaki,K. (1998) Two distinct kinds of tubular organelles involved in the rapid recycling and slow processing of endocytosed transferrin. *Biochem. Biophys. Res. Commun.*, **242**, 151–157.
Schirmbeck,R. and Reimann,J. (1996) 'Empty' Ld molecules capture peptides from endocytosed hepatitis B surface antigen particles for major histocompatibility complex class I-restricted presentation. *Eur. J. Immunol.*, **26**, 2812–2822.
Sheff,D.R., Daro,E.A., Hull,M. and Mellman,I. (1999) The receptor recycling pathway contains two distinct populations of early endosomes with different sorting functions. *J. Cell Biol.*, **145**, 123–139.
Slot,J.W., Geuze,H.J., Gigengack,S., Lienhard,G.E. and James,D.E. (1991) Immuno-localization of the insulin regulatable glucose transporter in brown adipose tissue of the rat. *J. Cell Biol.*, **113**, 123–135.
Sonnichsen,B., De Renzis,S., Nielsen,E., Rietdorf,J. and Zerial,M. (2000) Distinct membrane domains on endosomes in the recycling pathway visualized by multicolor imaging of Rab4, Rab5 and Rab11. *J. Cell Biol.*, **149**, 901–914.
Sprang,S.R. (1997) G protein mechanisms: insights from structural analysis. *Annu. Rev. Biochem.*, **66**, 639–678.
Sugita,M., Grant,E.P., van Donselaar,E., Hsu,V.W., Rogers,R.A., Peters,P.J. and Brenner,M.B. (1999) Separate pathways for antigen presentation by CD1 molecules. *Immunity*, **11**, 743–752.
Trowbridge,I.S., Collawn,J.F. and Hopkins,C.R. (1993) Signal-dependent membrane protein trafficking in the endocytic pathway. *Annu. Rev. Cell Biol.*, **9**, 129–161.
Verges,M., Havel,R.J. and Mostov,K.E. (1999) A tubular endosomal fraction from rat liver: biochemical evidence of receptor sorting by default. *Proc. Natl Acad. Sci. USA*, **96**, 10146–10151.
Walther,K., Krauss,M., Diril,M.K., Lemke,S., Ricotta,D., Honing,S., Kaiser,S. and Haucke,V. (2001) Human stoned B interacts with AP-2 and synaptotagmin and facilitates clathrin-coated vesicle uncoating. *EMBO rep.*, **2**, 634–640.
Yamashiro,D.J., Tycko,B., Fluss,S.R. and Maxfield,F.R. (1984) Segregation of transferrin to a mildly acidic (pH 6.5) para-Golgi compartment in the recycling pathway. *Cell*, **37**, 789–800.

Received February 18, 2002; revised and accepted April 10, 2002